13th World Conference on Earthquake Engineering
Vancouver, B.C., Canada
August 1-6, 2004
Paper No. 316

SEISMIC PERFORMANCE OF PLATE REINFORCED COMPOSITE COUPLING BEAMS

Wai Yin LAM[1], Ray Kai Leung SU[2], Hoat Joen PAM[3]

SUMMARY

An experimental research has been carried out on a newly proposed design of plate-reinforced composite (PRC) coupling beams. The design makes use of the composite action between structural steel and reinforced concrete (RC) by embedding a steel plate vertically into a conventional RC section with longitudinal flexural and transverse shear reinforcement. The composite action is enhanced by shear studs welded onto the steel plate along the longitudinal direction close to the flexural reinforcement. Shear studs are also welded on the plate in the anchorage regions in the wall piers to provide bearing to the plate.

A series of composite and conventional RC coupling beam specimens of span/depth ratio (l/h) 2.5 were tested under reversed cyclic loading to simulate seismic induced forces. Previous reports by the authors on some of the specimens have demonstrated a superior behavior of PRC coupling beams over conventional RC coupling beams under both elastic loading and inelastic deformations.

This paper presents the experimental results on three of the PRC coupling beams. One of them contained shear studs in the wall regions only, while the other two contained shear studs in both the beam and the wall regions. The difference between the latter two was that one of them contained longitudinal reinforcement of smaller diameters, which, however, formed the same total reinforcement area as that of the other two beams.

It was found that the absence of shear studs in the beam span would only slightly reduce the beam capacity without imposing much adverse effect on the inelastic performance under reversed cyclic loading. It was also found that the size of longitudinal reinforcement would affect the failure behaviors of coupling beams. Recommendations on the size of longitudinal reinforcement and shear stud arrangements for this new coupling beam design are then given.

---

[1] PhD Student, The University of Hong Kong, Pokfulam Road, Hong Kong, China
Email: wylam1@hkusua.hku.hk
[2] Assistant Professor, The University of Hong Kong, Pokfulam Road, Hong Kong, China
Email: klsu@hkucc.hku.hk
[3] Associate Professor, The University of Hong Kong, Pokfulam Road, Hong Kong,China
Email: pamhoatj@hkucc.hku.hk

INTRODUCTION

Coupled shear walls are common lateral load-resisting structural components in high-rise reinforced concrete (RC) buildings, in which the coupling beams spanning across the openings are normally the most critical elements. Because of architectural considerations and the need to accommodate service voids, these beams are usually of small dimensions, and small stiffness as compared with the wall piers in turn. Therefore, they often experience very high induced bending and shear stresses under lateral loads.

In order to remain elastic, so as to prevent yielding, under wind-induced reversed cyclic loading, conventional RC coupling beams with longitudinal flexural reinforcement and vertical shear reinforcement are made deep when large initial stiffness and shear capacities are required. However, they will be in danger of failing in a brittle way through the formations of diagonal shear or sliding cracks under earthquake-induced reversed cyclic loading if their span/depth ratio (l/h) is smaller than 1.5 [1, 2].

To ensure a sufficient shear capacity under large wind loading, especially in high-rise buildings, and survival of the structure under high intensity cyclic loading during an earthquake, alternative designs are required for improving the strength, stiffness, ductility and energy dissipation abilities of coupling beams. For this reason, various alternatives, like (1) composite coupling beams making use of structural steel beams embedded in nominally reinforced concrete [3, 4], diagonally reinforced coupling beams [5] and rhombic reinforcement layout [6], have been proposed. The authors also started the research on PRC coupling beams [7] with the aim of providing the construction industry with a feasible alternative design.

DESIGN OF PRC COUPLING BEAMS

Characteristics of PRC Coupling Beams

A PRC coupling beam contains a vertically embedded steel plate that spans across the beam and frames into the wall piers for anchorage. Shear studs are welded on both vertical faces of the plate along the top and the bottom longitudinal reinforcement throughout the span to enhance the plate/RC composite action in taking both shear and flexure. Shear studs are also provided in the wall regions to increase the plate bearing strength.

One of the major problems associated with conventional RC coupling beams is the formation of sliding shear cracks near the beam-wall joints under load reversals. These cracks inactivate the beam-wall shear transfer through the aggregate interlock action, causing brittle sliding failure. The embedded steel plate in a PRC coupling beam, however, provides a continuous medium for shear transfer even after serious concrete cracking near the beam-wall joints under inelastic deformations.
Figure 1 shows the reinforcement cage of the proposed PRC coupling beam applied in a private residential development project in Hong Kong.

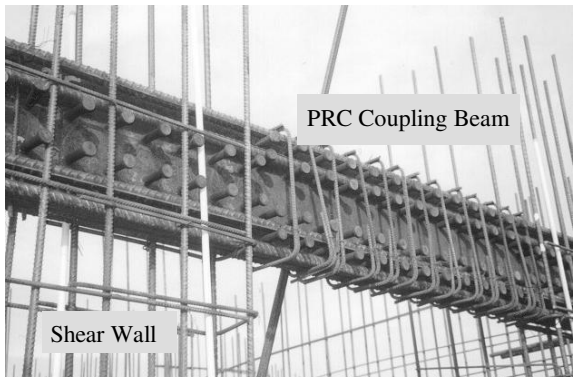

Figure 1. On-site Photo of PRC Coupling Beam Reinforcement Cage

Plate Anchorage Design in Wall Regions

Theoretically the anchorage of the steel plate is provided by the bearing stresses of concrete and shear studs, while the contributions of the plate surface friction is negligible and thus ignored. As the shear strength of the reinforced concrete was ignored in the preliminary design, the steel plate was designed to transfer all the shear forces (V_u) and part of the bending moments (i.e. the ultimate plate bending moment M_{up}) from the coupling beam to the shear walls at the beam-wall joints. These forces would be balanced by the bearing stresses on the plate in the wall regions. With the assumed uniformly distributed bearing stresses (w) as shown in Figure 2(a), the required anchorage length (L_a) of the plate was obtained based on vertical force and the moment equilibriums at ultimate limit state as follows:

$$L_a \geq L_1 + L_2 = 2\sqrt{\frac{M_{up}}{w} + \frac{V_u^2}{2w^2}} + \frac{V_u}{w}\text{, where } L_1 \text{ and } L_2 \text{ are values shown in the figure} \quad (1)$$

Based on the authors' experimental observations, and by welding more shear studs on the plate near the beam-wall interfaces, the model has been revised as a simplified stress distribution shown in Figure 2(b), where the design considers only the shear resistance provided by the plate ($V_{p,\ prov}$) instead of V_u. As smaller slips will be available at locations further away from the beam-wall interfaces, a triangular stress distribution is considered in Region II. Assuming a high degree of shear stud mobilization near the beam-wall interfaces, L_a can be revised as follows:

$$L_a \geq L_1 + L_2 = \frac{V_{p,prov}}{2w} + \frac{1}{2}\sqrt{\frac{12M_{up}}{11w} + \frac{3V_{p,prov}^2}{11w^2}} \quad (2)$$

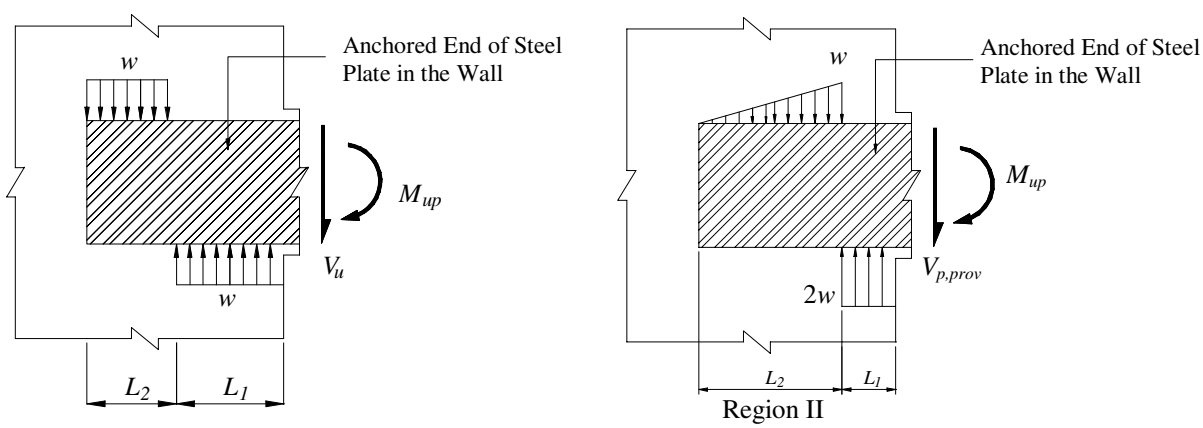

(a) Original Model (b) Revised Model

Figure 2. Proposed Models for Anchorage Design

EXPERIMENTAL PROGRAM

Test Specimens

The three coupling beams (l/h=2.5) discussed in this paper were the same geometrically, each with two identically reinforced large panels incorporated with its ends simulating part of the walls for investigating beam-wall interactions. Two base beams were also incorporated at the top and bottom ends of each 90°-rotated specimen for fixation onto the loading frame. The specimen dimensions and reinforcement details are shown in Figure 3, and the material properties in Table 1.

Each PRC coupling beam contained a 10mm thick Grade 50 steel plate that framed into the wall piers, where two rows of shear studs were welded on each face to enhance plate anchorage. The plates were of two different yield strengths (f_{yp}) as they were from two batches.

The shear links were identical in all the three beams and the longitudinal reinforcement areas were also the same. It was observed from the tests on Unit CF and some previous units [8,9] that comparatively large reinforcement bar sizes (about one-tenth of the smallest beam dimension) would result in bond-slip failure under large inelastic deformations although the bars had developed their full capacities prior to failure. Thus, smaller bar sizes were adopted in Unit CF2 in order to avoid this problem.

In order to identify the role of shear studs along the beam span, shear studs were absent in the beam span of Unit CW but were provided in the other two beams.

Note that the plate anchorages were designed based on the original proposed model, so uniformly distributed shear studs were provided.

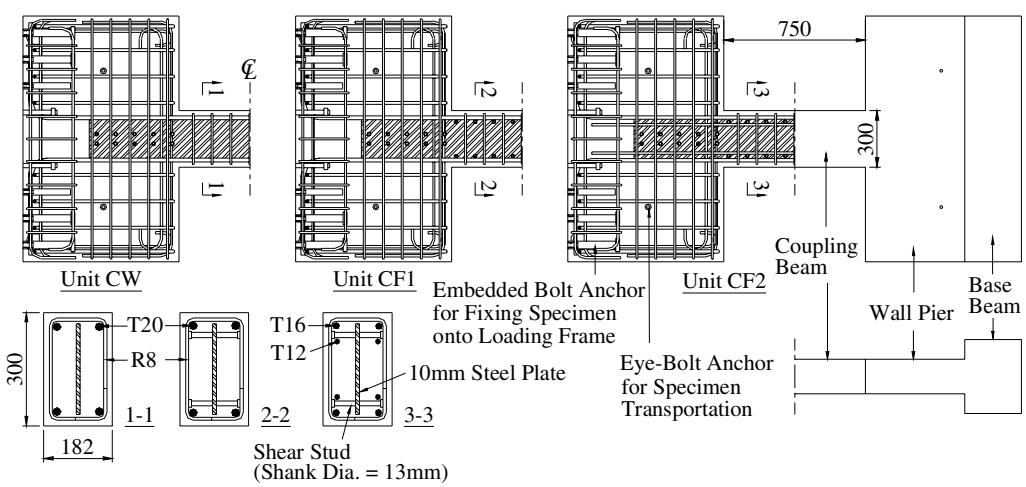

Figure 3. Specimen Dimensions and Reinforcement Details

Table 1. Material Properties

Specimen	f_y (T20)	f_y (T16)	f_y (T12)	f_{yv} (R8)	f_{yp}	f_{cu} (Test-Day)	f_c' (Test-Day)
Unit CW	514	N/A	N/A	392	435	53.7	50.2
Unit CF1	523	N/A	N/A	367	435	51.9	48.1
Unit CF2	N/A	541	507	392	370	48.3	45.8

Notes: All units are in MPa.
f_y = yield strength of longitudinal reinforcement
f_{yv} = yield strength of transverse reinforcement
f_{cu} = cube strength of concrete
f_c' = cylinder strength of concrete

Loading Applications

Test Setup

Figure 4 shows the test setup, which was designed by Kwan and Zhao [10], and the loading application. Loading was applied from a 500kN actuator to the top end of each 90°-rotated specimen through a rigid arm with the line of action passing through the beam center. This way, the coupling beam was loaded with a constant shear force along the span and a linearly varying bending moment with the contra-flexure point at mid-span. In order to simulate the real situation in which the wall piers at the two ends of a coupling beam remain parallel under deflections of the building, a parallel mechanism was installed to connect the upper rigid arm with the lower structural steel beam fixed on the floor.

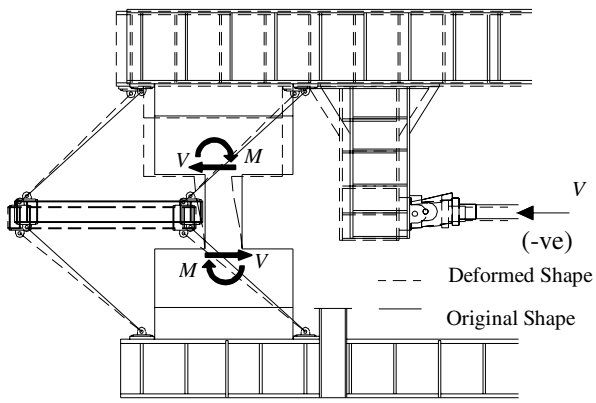

Figure 4. Loading Frame and Loading Application

Loading History

Reversed cyclic loading was first applied to each specimen in a load-controlled cycle up to 75% of the theoretical ultimate shear capacity (V_u^*) to obtain the yield rotation (θ_y) for ductility factor (μ) 1 by the 4/3 rule, where the beam rotation (θ) was defined as the differential displacement between the two beam ends in the loading direction divided by the clear span (l). The specimen was then displaced to $\mu = \pm 1$ for one cycle, then to each successive ductility factor for two cycles (Figure 5). The test was terminated when the peak load reached in the first cycle of a ductility level fell below the lesser of $0.8V_u^*$ and 80% of the maximum measured shear (V_{max}), and the specimen was then considered to have failed.

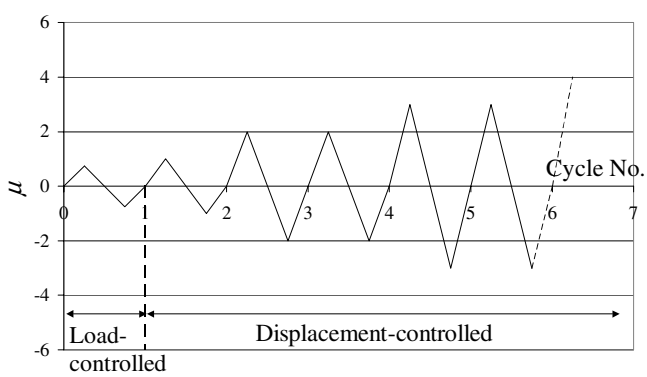

Figure 5. Loading History

Instrumentations
The specimens were instrumented with linear variable displacement transducers (LVDTs) to capture the deflection and curvature profiles, as well as and strain gauges on the plates, longitudinal bars, stirrups and some of the shear studs to investigate the internal load distributions.

RESULTS AND DISCUSSIONS

Overall Performance
The experimental results are summarized in Table 2 below. Units CF1 and CF2 developed a higher percentage of strength above the theoretical value than Unit CW, suggesting that the shear studs in the beam span might have enhanced the plate/RC composite action. Unit CF2 was loaded to a maximum shear stress (v_{max}) of 9.2MPa while the RC component was designed to take up about 2.5MPa only. This was far above the limit of 5MPa given in BS8110 [11] for conventional RC beams.

Table 2. Summary of Experimental Results

Specimen	V_{max}	v_{max}	V_{max}/V_u^*	θ_y	θ_u	μ_u
	kN	MPa		Rad	Rad	
Unit CW	397	8.2	1.18	0.0104	0.0499	4.8
Unit CF1	417	8.6	1.33	0.0100	0.0850	8.5
Unit CF2	434	9.2	1.35	0.0089	0.0562	6.3

Notes: θ_u = ultimate measured rotation of beam
μ_u = ultimate measured ductility

Figure 6 shows the coupling beams after test. Plastic hinges can be easily observed in all the three PRC coupling beams, but those in Unit CW shifted away from the beam-wall joints into the beam span as compared with those in the other two units. This could have been due to the comparatively stronger fixation of the plate in the walls than in the beam in this unit due to the absence of shear studs in the beam span.

The crack patterns in all the three specimens were similar before the peak loads were reached at the second ductility level (i.e. $\mu = 2$), where shear cracks were dominant at positions of the plastic hinges formed later, and small flexural shear cracks could be observed along the longitudinal reinforcement. However, after reaching the peak loads, bond-slip cracks started to govern in Units CW and CF1, leaving the central regions uncracked throughout the tests, while flexural shear cracks continued to develop and propagate towards the central region in Unit CF2 although traces of bond-slip problems could still be found. Therefore, bar sizes below one-tenth of the smallest beam dimension should be adopted in order to fully utilize every part of a short RC beam.

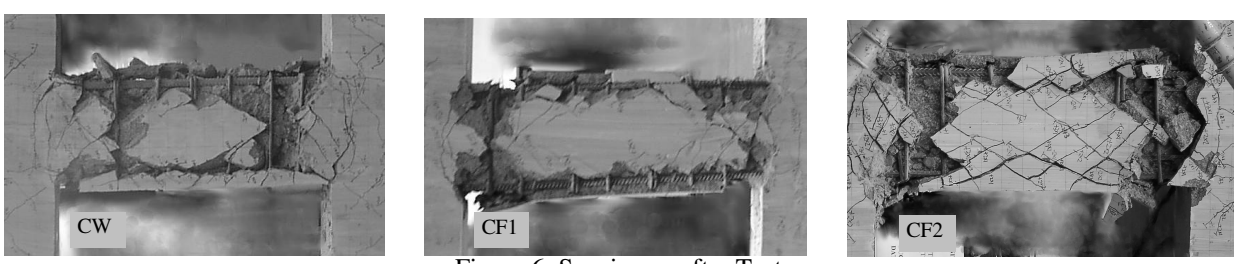

Figure 6. Specimens after Test

Load-Rotation Responses
The load-rotation (V-θ) responses of all the three specimens were similar as can be seen in Figure 7. This, together with previous observation that a PRC beam with a plain plate could not give ductile hysteretic

response [9], shows that the plate anchorage in the walls piers is of vital importance to the post-elastic performance.

Although the shear studs in the beam span seemed to have little effect on the beam performance, the larger capacities developed in Units CF1 and CF2 compared with Unit CW, as shown in the normalized envelopes that eliminate the pre-existing difference due to the varying material strengths, suggest that these shear studs would help to develop a higher degree of composite action, i.e. a better utilization of the components, in the coupling beam.

The improvement in Unit CF2 as compared with Unit CF1 contributed by the reduction of bar sizes could not be easily observed from the load-rotation curves. However, the strength and stiffness dropped considerably in Unit CF1 after reaching the peak load at μ = 2 probably due to bond-slip in the longitudinal reinforcement while Unit CF2 maintained almost the same strength with a smaller stiffness degradation at the next stage. Thus, the prevention of bond-slip could help to delay the strength and stiffness degradations.

It should be noted that the peak load had not fallen below the defined failure load before the test was terminated due to jack failure. Therefore, Unit CF1 could have undergone more cycles if the accident had not happened.

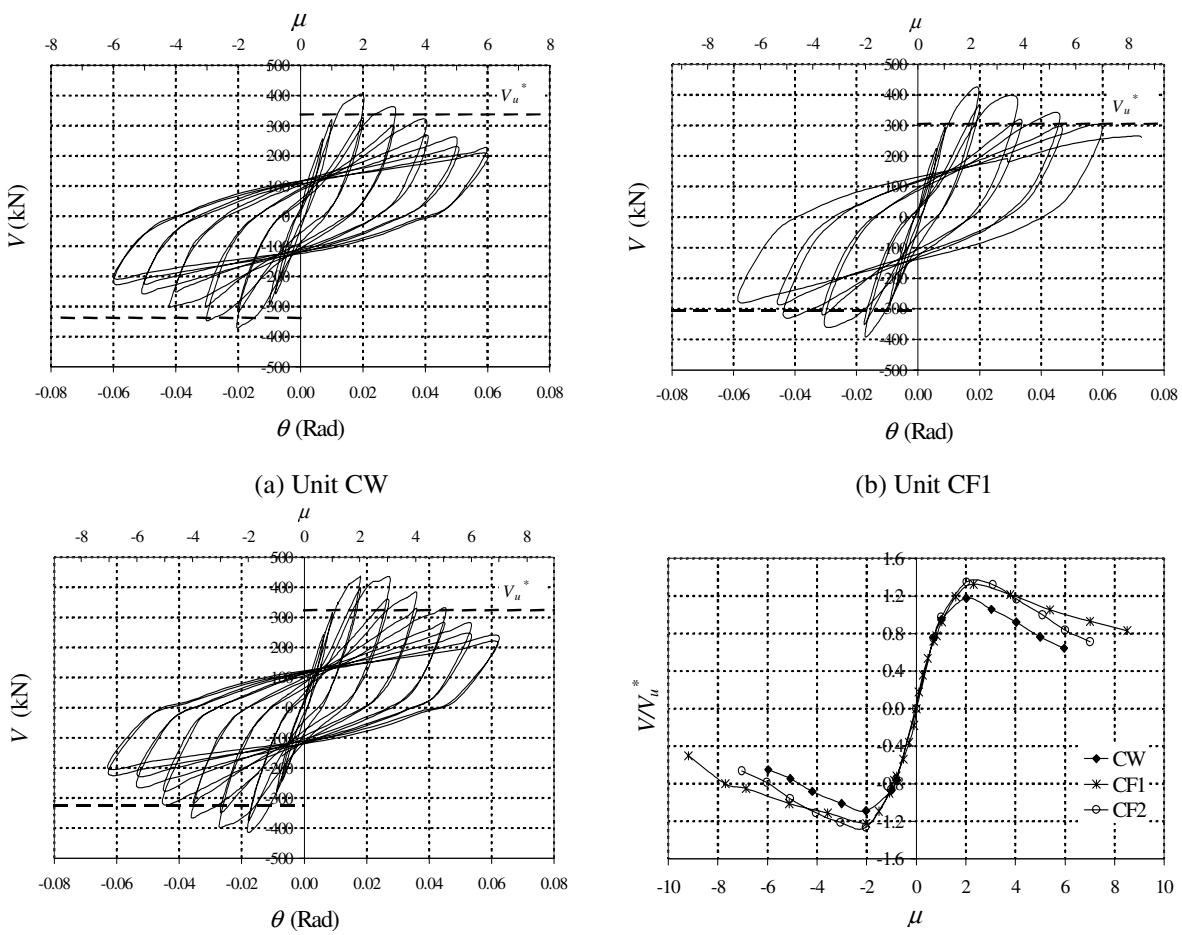

(a) Unit CW (b) Unit CF1

(c) Unit CF2 (d) Normalized Envelopes

Figure 7. Load-Rotation Curves of Coupling Beams

Energy Dissipations

In Figure 8, the cumulative energy dissipated ($W_{d,cum}$) is normalized by the energy dissipated in the yield cycle ($W_{d,y}$) for a fair comparison between the energy dissipation abilities of the three PRC coupling beams. With the embedded steel plates, the specimens showed steady energy dissipation abilities. The cumulative energy dissipated in Unit CW was the smallest at any post-elastic stage among the three, while the energy dissipation abilities were similar for Units CF1 and CF2. This further indicates that the shear studs in the beam span are contributive to the improved post-elastic performance. As Unit CF2 underwent more load cycles than Unit CF1, it could dissipate much more energy than the latter. The difference might have partly been due to the prevention of bond-slip in Unit CF2, although the major reason for the difference could have come from the accident happening on Unit CF1 mentioned above.

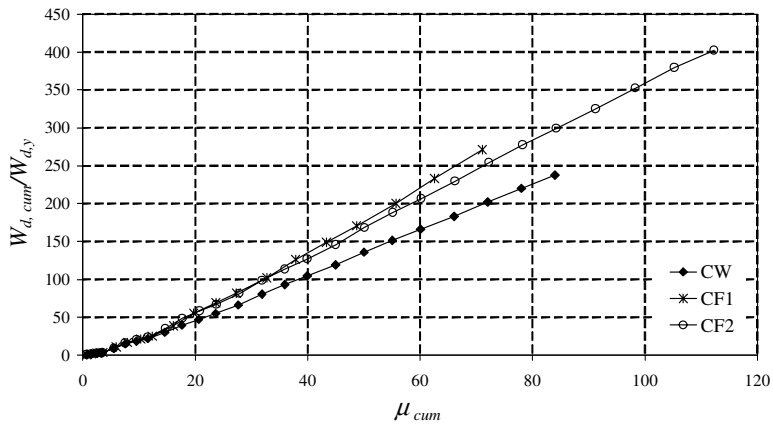

Figure 8. Normalized Cumulative Energy Dissipated

Strength Degradations

Figure 9 shows the strength degradations in repeated cycles at each ductility level. The damage in the concrete, especially at early stages, could have accounted for the major part of the loss in strength, but the weakened plate/RC interaction that resulted in smaller contribution of the plates might be another source of strength degradations.

Unit CW experienced the largest strength degradation (over 15%) after undergoing the first inelastic cycle, indicating that it had suffered the most serious damage among the three specimens at this stage. This was probably due to the weakest plate/RC interaction that resulted in the smallest contribution of the embedded steel plate. As the applied load and the induced beam rotation increased, the interface shear required to bond the plate with the surrounding RC would have increased beyond the natural plate/RC bond available. The weakened bond would result in a smaller amount of shear transferred to the plate from the RC when the load cycle was repeated at $\mu = 2$, thus causing a greater strength degradation.

The strength degradations in repeated cycles decreased as the ductility levels increased in all the specimens. This was probably due to the diminishing role the RC was playing as the induced beam rotation increased, so that damages to the concrete in the first cycle would not reduce the overall strength significantly.

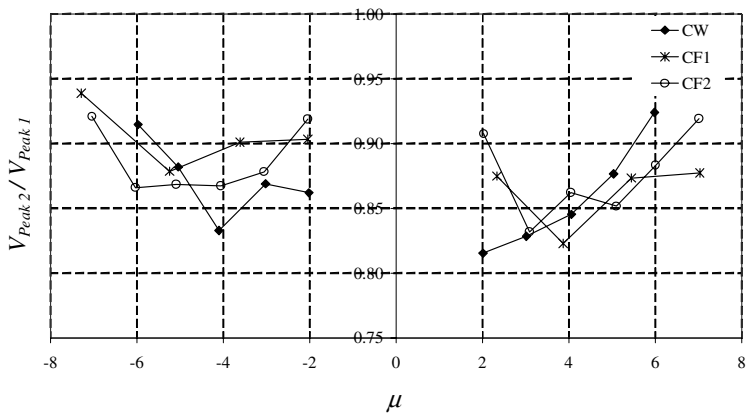

Figure 9. Strength Retentions in Repeated Cycles

Strain Distributions

The strain distributions along the top fibers of the plates and the top longitudinal reinforcement at the peak of the first cycle at each positive ductility level are shown in Figures 10 and 11 respectively. As a considerable number of strain gauges were damaged after reaching μ = 3, strain profiles are only shown up to this stage.

While the strain profiles were anti-symmetrical about the beam center in the steel plates, the points of zero strain in the longitudinal bars, and the point of contraflexure in the RC in turn, continued to shift towards the compression end during the tests. Such difference, together with the difference in the order of strain magnitudes, between the steel plates and the RC suggests that there were both longitudinal and transverse plate/RC interface slips that resulted in different neutral axis positions and curvatures of plate and RC sections respectively. In fact, interface slips are unavoidable when the natural plate/RC bond is smaller than the required interface shear because shear studs can only be mobilized by interface slips. However, once the shear studs are mobilized, they can enhance the interface shear transfer, thus preventing further relative slips.

Although all the longitudinal bars had yielded near the beam-wall joints after reaching the peak of the first inelastic cycle, only those in Unit CF2 continued to deform further. This phenomenon was consistent with the observation from the crack patterns that bond-slips happened in the longitudinal reinforcement of Units CW and CF1, inhibiting them from deforming further with the concrete as the induced beam rotations increased.

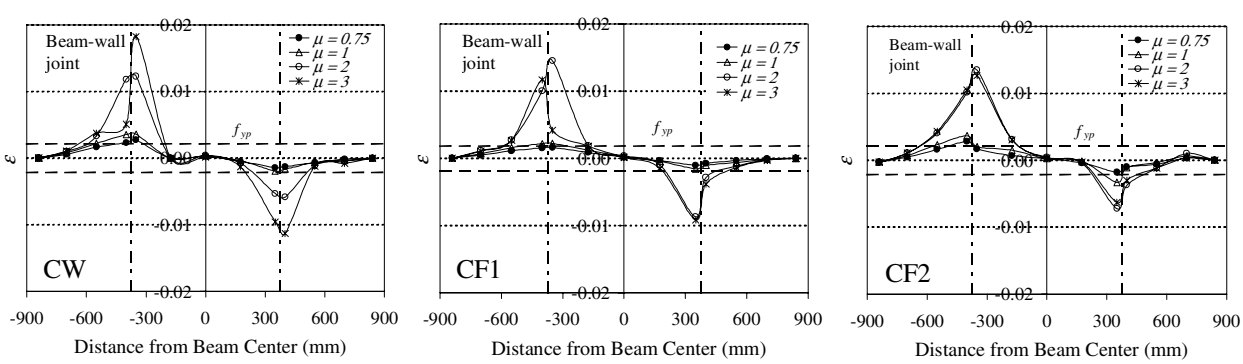

Figure 10. Strain Distribution along Top Fibers of Steel Plates

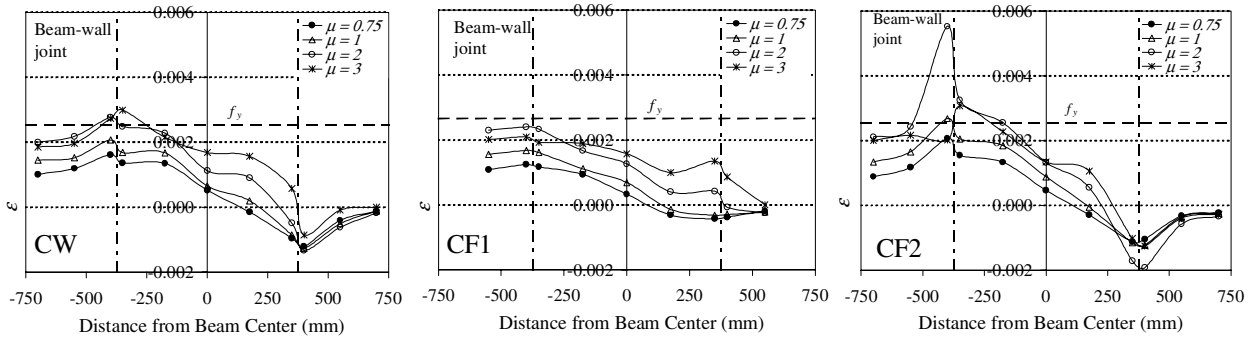

Figure 11. Strain Distribution along Top Longitudinal Reinforcement

CONCLUSIONS

The basic design principles of PRC coupling beams has been introduced and the experimental results of the reversed cyclic loading tests on three PRC coupling beam specimens reported in this paper. The following conclusions are drawn from the experimental observations:

1. A PRC coupling beam can effectively resist both considerable elastic loading and inelastic deformations provided that the embedded steel plate can be firmly anchored in the wall piers.
2. Shear studs in the beam span can enhance the plate/RC interaction, which will in turn improve the post-elastic beam performance, although their absence would not significantly reduce the effectiveness of this coupling beam design.
3. Longitudinal bar sizes larger than one-tenth of the smallest beam dimension may result in bond-slip failure under large deformations in short and medium beams, although the reinforcement may still develop their full strengths.

ACKNOWLEDGEMENTS

The research described here has been supported by The University of Hong Kong through the Large Item Grant by Research Grants Council of Hong Kong SAR (Project No. HKU7129/03).

REFERENCES

1. Paulay T. 1971. Coupling Beams of Reinforced Concrete Shear Walls. *Proceedings of ASCE* 97(ST3): 843 – 862.
2. Wang W., Fu X. & Ni Y. 1992. Behavior of Ceramite Concrete Coupling Beams in Shear Wall Structure under Reversed Cyclic Loading (in Chinese). *Journal of Building Structures* 13(1): 71 – 78.
3. Gong B., Shahrooz B.M. and Gillum A.J. (1996), "Seismic Behaviour and Design of Composite Coupling Beams", *Proceedings of the Engineering Foundation Conference on Composite Construction in Steel and Concrete III,* 9-14 June 1996, ASCE, pp. 258 – 271.
4. Gong B. and Shahrooz B.M. (2001a), "Concrete-steel Composite Coupling Beams I: Component Testing", *Journal of Structural Engineering*, ASCE, Vol. 127, No. 6, June 2001, pp. 625 – 631.
5. Paulay T. & Binney J.R. 1974. Diagonally Reinforced Coupling Beams of Shear Walls. *ACI Special Publication* SP42: 579 – 598.
6. Tegos I.A. & Penelis G.G. 1988. Seismic Resistance of Short columns and Coupling Beams Reinforced with Inclined Bars. *ACI Structural Journal* 85(1): 82 – 88.
7. Lam W.Y., Su R.K.L. & Pam H.J. 2001. Embedded Steel Composite Coupling Beams – a New Proposal. *Proceedings of International Conference on Construction 19-21 June 200*1 2: 93 – 104.

8. Lam W.Y., Su R.K.L. and Pam H.J. (2003), "Strength and Ductility of Embedded steel Composite Coupling Beams", *International Journal of Advances in Structural Engineering*, Vol. 6, No. 1, 2003, pp. 23-35.
9. Lam W.Y., Su R.K.L. & Pam H.J. 2002. The Performance and Design of Embedded Steel Composite Coupling Beams. *Proceeding of Structural Engineers World Congress 9-12 October 2002* (in CD Rom).
10. Kwan A.K.H. and Zhao Z.Z. (1998), "Non-linear Behaviour of Reinforced Concrete Coupling Beams", *The Fifth International Conference on Tall Buildings*, Hong Kong, 1998, pp. 410 – 415.
11. BSI 1985. *BS8110, Part 1, Code of Practice for Design and Construction.* British Standards Institution 1985, London.